Joint Gain and Timing Recovery With Applications to Magnetic Tape Storage

Jaekyun Moon, *Fellow, IEEE*, Jaewook Lee, and Daejung Yoon

Department of Electrical and Computer Engineering, University of Minnesota, Minneapolis, MN 55455 USA

We discuss a joint gain and timing recovery scheme that provides performance advantages in tape recording environments plagued by deep amplitude fades and timing error fluctuations. The idea is to find a particular combination of the gain and phase errors that best matches with a window of playback samples and use the resulting estimates to drive the automatic gain control (AGC) loop and the timing recovery loop. The gain and phase estimate pair is obtained and maintained separately for each survivor path in the Viterbi processor, and is used to compensate for the corresponding distortions in the Viterbi branch metric computation. The gain and phase error estimates are then taken out of the best survivor path possibly with some delay and are used to drive the respective loops. The BER performance and cycle slip probabilities are compared with those of a conventional AGC and timing recovery scheme.

***Index Terms*—Automatic gain control, dropouts, inter-symbol interference, phase-locked loop, synchronization, timing recovery.**

I. Introduction

OCCASIONAL amplitude fades known as "dropouts" are a notable source of bit errors in magnetic tape recording [1], [2]. The dropouts are usually caused by the media defects or the loose particles in the head-to-media interface, effectively increasing the head-tape spacing momentarily. The head-tape spacing increase in turn results in an exponential loss in the playback signal strength. Sampling phase errors, which are inevitable in practical systems, also contribute to the system failure, especially as the signal-to-noise ratio (SNR) drops.

In this paper, we develop a detection scheme well suited to the fading tape channel environment, making use of a window-based joint gain/phase estimator that operates in conjunction with a Viterbi detector. The proposed joint estimation is based on finding a particular combination of the gain and phase errors, along each survivor path, that best matches with the playback samples collected over a finite window. In essence, the gain and phase error estimate trajectories are obtained and updated separately for each survivor data path; the gain and phase error estimates associated with the best survivor path are then released with some delay to the global automatic gain control (AGC) loop and the phase-locked loop (PLL), respectively.

The bit-error rate (BER) performance and cycle slip probabilities are compared with those corresponding to a conventional AGC and timing recovery scheme, assuming the presence of repetitive dropouts and time-varying sampling phase error in the captured playback signal. The conventional scheme here refers to the AGC and timing loops that operate based on traditional, disjoint estimation of gain and timing errors. The simulation results indicate that the proposed scheme enables the read channel to operate at a significantly lower channel SNR than the conventional AGC and timing recovery loops.

II. Channel Model and Joint Gain/Phase Estimation

In Fig. 1(a), a binary sequence x_k is converted into a continuous-time impulse train with the impulses occurring at a rate of $1/T$, where T denotes the symbol period. The continuous-time signal goes through the intersymbol interference (ISI) channel impulse response $h(t)$. In the context of magnetic recording, $h(t)$ represents the "dibit" response. The ISI channel output is distorted by an amplitude fluctuation function $\lambda(t)$ and then additive Gaussian noise (AWGN) $w(t)$. The distorted signal is filtered by the front-end filter $p(t)$ and sampled at time $t = kT + \Delta_k$ to result in the received signal c_k. Here Δ_k represents the sampling phase error, the error between the write clock phase and the read clock phase. The discrete-time equivalent model that results from the first-order approximation of the timing error effect is shown in Fig. 1(b), where the filtered and sampled playback signal is given by

$$\begin{aligned} c_k &\approx \lambda_k \sum_j f_j x_{k-j} + \lambda_k \Delta_k \sum_j g_j x_{k-j} + n_k \\ &= \lambda_k y_k + \lambda_k \Delta_k \varepsilon_k + n_k \end{aligned} \tag{1}$$

where $f_j = h(t) * p(t)|_{t=jT}$ is the impulse response of the effective discrete-time channel with the front-end filter $p(t)$, $n_k = w(t) * p(t)|_{t=kT+\Delta_k}$ is the filtered and sampled version of AWGN $w(t)$, $g_j = h'(t) * p(t)|_{t=jT}$, and $\lambda_k = \lambda(t)|_{t=kT+\Delta_k}$. Note that $\{g_j\}$ in general contains non-causal components even when $\{f_j\}$ does not. The second term arises due to the sampling phase error, and the parameters λ_k and Δ_k appear together in a tightly coupled, multiplicative form. We comment that although the algorithm development is based on the first-order model, the actual simulation results presented later do not make such approximation. Thus, the validation of the algorithm through simulation points to the reasonable accuracy of the first-order phase error model for our purposes. We also mention that the amplitude fade model used here is very crude in the sense that fading due to head-tape separation should actually be modeled as a frequency-dependent phenomenon [1], [2].

The traditional gain error and phase error estimators operate in a disjoint fashion, with each estimator targeting only the gain error or timing error estimation. However, since λ_k and Δ_k appear tightly coupled together, as seen in (1), the disjoint estimators are distinctly suboptimal. This is because any uncompensated error from one estimator has a direct impact on the quality of the estimate for the other estimator.

Digital Object Identifier 10.1109/TMAG.2007.893529

Color versions of one or more of the figures in this paper are available online at http://ieeexplore.ieee.org.

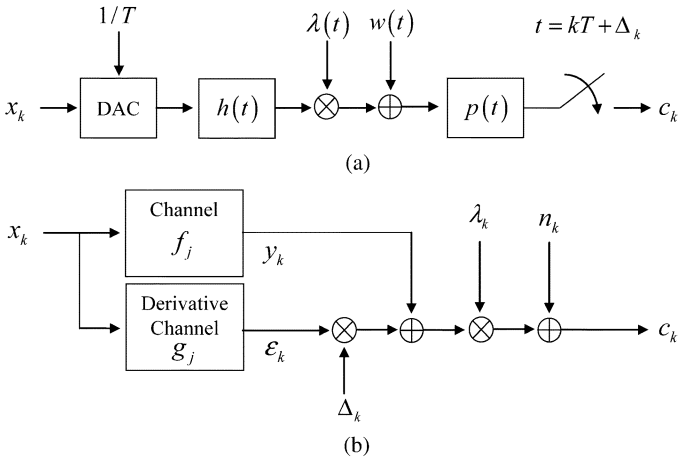

Fig. 1. Block diagrams of channel models. (a) Continuous-time channel model (b) Discrete-time channel model.

To improve estimation quality relative to this traditional method, we perform joint, simultaneous estimation of λ_k and Δ_k. Assume that a window of M observation samples from time $k - M + 1$ to time k to be utilized in estimation. Introducing a vector notation $\mathbf{c}_k = [c_{k-M+1}, \ldots, c_k]'$, $\boldsymbol{\varepsilon}_k = [\varepsilon_{k-M+1}, \ldots, \varepsilon_k]'$ and likewise for $\mathbf{y}_k$ and $\mathbf{n}_k$, we write

$$\begin{aligned}\mathbf{c}_k &\approx \lambda_k \mathbf{y}_k + \gamma_k \boldsymbol{\varepsilon}_k + \mathbf{n}_k \\ &= [\mathbf{y}_k \quad \boldsymbol{\varepsilon}_k] \begin{bmatrix} \lambda_k \\ \gamma_k \end{bmatrix} + \mathbf{n}_k \end{aligned} \tag{2}$$

where $\gamma_k \triangleq \lambda_k \Delta_k$ and the approximation is based on the assumptions: $\lambda_k \approx \lambda_{k-1} \approx \cdots \approx \lambda_{k-M+1}$ and $\Delta_k \approx \Delta_{k-1} \approx \cdots \approx \Delta_{k-M+1}$.

Letting the error vector $\mathbf{e}_k \triangleq \mathbf{c}_k - [\mathbf{y}_k \boldsymbol{\varepsilon}_k][\lambda_k \gamma_k]'$, the least squared error (LSE) solution that minimizes its squared norm is given by

$$\begin{bmatrix} \hat{\lambda}_k \\ \hat{\gamma}_k \end{bmatrix} = \mathbf{K}^{-1} \begin{bmatrix} \mathbf{y}_k{}' \\ \boldsymbol{\varepsilon}_k{}' \end{bmatrix} \mathbf{c}_k \tag{3}$$

where

$$\mathbf{K} = \begin{bmatrix} \mathbf{y}_k{}' \cdot \mathbf{y}_k & \mathbf{y}_k{}' \cdot \boldsymbol{\varepsilon}_k \\ \boldsymbol{\varepsilon}_k{}' \cdot \mathbf{y}_k & \boldsymbol{\varepsilon}_k{}' \cdot \boldsymbol{\varepsilon}_k \end{bmatrix}. \tag{4}$$

In order to find the unique solution, the matrix K must be invertible. Inverting K becomes numerically unstable if the off-diagonal elements of K become large. It turns out that as we increase the window size M, the channel output vector $\mathbf{y}_k$ and the derivative channel output vector $\boldsymbol{\varepsilon}_k$ become increasingly uncorrelated, making the dot products $\boldsymbol{\varepsilon}_k{}' \cdot \mathbf{y}_k$ and $\mathbf{y}_k{}' \cdot \boldsymbol{\varepsilon}_k$ approach zero. However, increasing M also results in the loss of ability to follow quickly varying parameters. Therefore, it is important to strike a good balance between the estimation quality and the tracking ability in empirically finding a reasonable value for M.

The estimates $\hat{\lambda}_k$ and $\hat{\gamma}_k$ can form the basis of the AGC and the timing recovery loops. The simplest way to get an estimate for $\hat{\Delta}_k$ would be to divide the estimate for the coupled parameter, $\hat{\gamma}_k$, by $\hat{\lambda}_k$.

III. Modifying the Viterbi Processor

The vectors $\mathbf{y}_k$ and $\boldsymbol{\varepsilon}_k$ are specific to the local input pattern. While they can be obtained for a path of decisions that are already released by the detector, we opt to incorporate the joint gain/phase estimation process into the Viterbi processor. To bring the estimation process inside the Viterbi processor, the state variable needs be defined based on enough input samples so that both $y_k = (x * f)_k$ and $\varepsilon_k = (x * g)_k$ are completely determined for a given branch. The need to specify ε_k results in an increased trellis size, as the "derivative" channel g_k is typically longer than the main channel response f_k. While the trellis size might be reduced with only a small loss of performance using local decision feedback, for the simulation results presented in this paper, we use a 32-state trellis versus the original 8-state extended class 4 partial response (EPR4) trellis, by considering one noncausal sample g_{-1}as well as causal samples up to g_4 in constructing ε_k for each branch.

In the beginning of each symbol cycle, $\hat{\lambda}_k$ and $\hat{\gamma}_k$ are updated for each trellis branch by using (3) based on $\mathbf{y}_k$ and $\boldsymbol{\varepsilon}_k$ obtained from the corresponding survivor path history. Next, each branch metric is computed according to

$$m_k = [c_k - \hat{\lambda}_k y_k - \hat{\gamma}_k \varepsilon_k]^2. \tag{5}$$

Note that the incorporation of the timing error estimate into the Viterbi processor in this fashion has already been considered in [3], while the concept of formulating the entire PLL as well as the sampling device along each survivor path has been investigated in [4].

After branch metrics are computed, competing paths merging into the same node get arbitrated as usual, and as a result, the survivor path is determined and updated for that node. As an extra step, both the $\hat{\lambda}_k$ and $\hat{\gamma}_k$ trajectories also get updated and stored in the memory. Before the end of the symbol processing cycle, $\hat{\lambda}_k$ and $\hat{\Delta}_k$ (obtained by dividing $\hat{\gamma}_k$ by $\hat{\lambda}_k$) associated with the best survivor path is released (with a judicious delay) to the global AGC and timing recovery loops that reside outside the Viterbi processor. The delay is determined by considering the tradeoff between the estimation accuracy and the loop stability.

The complexity and memory increase of the proposed scheme per node are relatively small, compared to the conventional scheme, especially because the latency associated with releasing $\hat{\lambda}_k$ and $\hat{\Delta}_k$ to the global loops is very small in practice. But the increased complexity burden comes mainly from the fourfold increase in the trellis size, as discussed above.

IV. Simulation Environment and Results

In order to compare the performance of the proposed loops with the conventional loops, traditional zero-forcing (ZF) gain estimator [5] and Mueller and Muller (M&M) phase estimator [6] are considered. For the gain recovery, the gain compensation factor κ_k of an AGC loop is given by

$$\kappa_k = \kappa_{k-1} + \mu \chi_k \tag{6}$$

where χ_k denotes the output of the gain error estimator and μ denotes the adaptation step size. For the ZF gain estimator, the gain error estimate χ_k is given by

$$\chi_k = (y_{k-\xi} - r_{k-\xi}) y_{k-\xi} \tag{7}$$

where ξ denotes the estimation latency and r_k denotes the gain-adjusted playback signal $\kappa_k c_k$. For the proposed joint estimator, the gain error estimate χ_k is given by

$$\chi_k = 1 - \hat{\lambda}_{k-\xi} \tag{8}$$

where $\hat{\lambda}_k$ is obtained from (3), with an understanding that c_k's are now gain-adjusted playback samples; $\hat{\lambda}_k$ will converge to 1 as the gain recovery loop goes to the steady state. Apparently, χ_k in (8) can serve as the gain error gradient necessary to drive the AGC loop.

For the timing recovery loop, the phase error estimate $\hat{\Delta}_k$ is filtered by a discrete-time loop filter and passed to an integrator. The output of the integrator feeds the interpolator that also takes input from an asynchronous, over-sampled analog-to-digital converter (ADC). The integrator output τ_k is given by

$$\tau_k = \tau_{k-1} + (\alpha\hat{\Delta}_{k-\xi} + I_k) \tag{9}$$

where $I_k = I_{k-1} + \beta\hat{\Delta}_{k-\xi}$, and α and β are the phase and frequency update gains of the loop filter, respectively.

For the well-known M&M phase estimator, $\hat{\Delta}_k$ is given by

$$\hat{\Delta}_k = r_{k-\xi}y_{k-\xi-1} - r_{k-\xi-1}y_{k-\xi} \tag{10}$$

where r_k denotes the gain/phase-adjusted playback samples. For the proposed joint estimator, $\hat{\Delta}_k$ is obtained from (3) with c_k's replaced by their gain and phase adjusted versions. Data decisions are made by the Viterbi detector with decision latency ω. Typically $\omega > \xi$.

In our simulation, the playback signal is the result of driving the ideal minimum-band EPR4 signal with random binary data frames with each frame containing 4096 bits. A sinusoidal timing-varying sampling phase error is imposed which swings from $-0.2T$ to $+0.2T$ with a period of $2000T$. The multiplicative distortion $\lambda(t)$ is modelled as a repetitive pattern of half-cycle sinusoids separated by flat regions. The amplitude of $\lambda(t)$at the deepest fade is set at 0.7 while the duration of each fade is $1000T$ with separation between successive fades also set to $1000T$. The two time-varying functions are aligned such that a peak of the phase error coincides with the amplitude dip. The SNR is defined as $E[y_k^2]/E[n_k^2]$ in the flat gain region with y_k and n_k as given in (1).

Fig. 2(a) shows that the proposed scheme can operate at lower SNRs than the conventional scheme based on disjoint operations of the ZF AGC and M&M timing loops. One important reason behind the improved BER is a reduced probability of cycle-slips, which cause burst errors in a frame [7]. The cycle-slip probabilities of the two schemes are compared in Fig. 2(b), where the cycle slip probability is defined as the number of frames having at least one cycle slip divided by the total number of frames. Enhanced robustness of the proposed scheme against cycle slips is evident. The operability at low SNRs is important as the channel operating conditions will become increasingly poor given the continuous demand for density improvement.

The loop filter coefficients α and β, the adaptation gain μ and the latency parameter ξ are adjusted to minimize the BER for each scheme at SNR $= 6$ dB. For the traditional ZF gain recovery and M&M phase recovery loops, the loop parameters are chosen as $\xi = 11$, $\omega = 80$, $\mu = 5.0 \times 10^{-2}$, $\alpha = 1.5 \times 10^{-2}$, and $\beta = 1.5 \times 10^{-4}$. For the proposed joint recovery loops, the loop parameters are set to $M = 30$, $\xi = 2$, $\omega = 80$, $\mu = 5.0 \times 10^{-4}$, $\alpha = 3.5 \times 10^{-4}$, and $\beta = 3.5 \times 10^{-6}$.

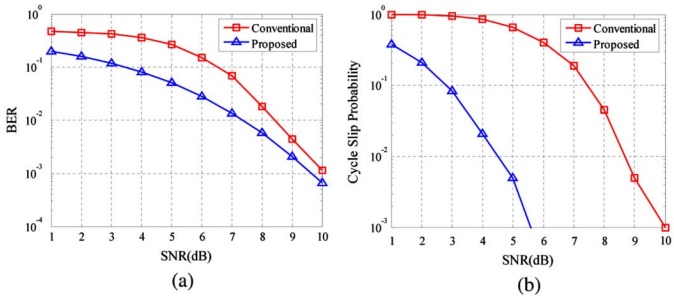

Fig. 2. Performance comparisons. (a) BER results. (b) Cycle slip probability.

V. Conclusion

It has been shown that the gain error and sampling phase error appear in the playback signal in a tightly coupled form. An improved joint gain/phase estimator has been proposed that simultaneously estimates the gain and sampling phase errors over a finite observation window. The joint estimator has been brought inside the Viterbi processor so that estimation is performed along each survivor path without latency. The branch metric computation now takes into account the distortion caused by the residual gain and phase errors in the signal that enters the Viterbi detector. Separate gain and gain–phase product estimate paths are maintained and updated along with each Viterbi survivor path. The gain and phase estimates taken out of the best survivor path feed the global AGC and timing loops, respectively. At the expense of increased Viterbi processing requirements, the proposed scheme offers improved BER performance and enhanced robustness against cycle slips.

Acknowledgment

This work was supported in part by the INSIC TAPE Program.

References

[1] F. Sarigoz, G. Li, B. V. K. V. Kumar, J. Bain, and J. Zhu, "Analysis of dropout peakshift in magnetic tape recording," *IEEE Trans. Magn.*, vol. 36, no. 5, pp. 2170–2172, Sep. 2000.

[2] B. Steingrimsson and J. Moon, "Dropout compensation in magnetic tape channels by adaptive equalization and coding," *IEEE Trans. Magn.*, vol. 37, no. 6, pp. 3981–3993, Nov. 2001.

[3] J. Moon and J. Lee, "Joint timing recovery and data detection with applications to magnetic recording," *IEEE Trans. Magn.*, vol. 42, no. 10, pp. 2576–2578, Oct. 2006.

[4] P. Kovintavewat, J. R. Barry, M. F. Erden, and E. Kurtas, "Per-survivor timing recovery for uncoded partial response channels," in *Proc. IEEE ICC*, 2004, pp. 2715–2719.

[5] J. W. M. Bergmans, *Digital Baseband Transmission and Recording*. Boston, MA: Kluwer Academic, 1996.

[6] K. Mueller and M. Muller, "Timing recovery in digital synchronous data receivers," *IEEE Trans. Commun.*, vol. COM-24, no. 5, pp. 516–531, May 1976.

[7] J. Liu, H. Song, and B. V. K. Vijaya Kumar, "Bound for loss of lock rate in partial response recording channels," *Electron. Lett.*, vol. 38, no. 16, pp. 928–930, Aug. 2002.

Manuscript received November 1, 2006; revised February 13, 2007 (e-mail: leex2244@umn.edu).